Cell volume regulation modulates NLRP3 inflammasome activation

Vincent Compan[1], Alberto Baroja-Mazo[2], Gloria López-Castejón[1], Ana I. Gomez[2], Carlos M. Martínez[2], Diego Angosto[3], María T. Montero[4], Antonio S. Herranz[4], Eulalia Bazán[4], Diana Reimers[4], Victoriano Mulero[3] and Pablo Pelegrín[1,2]

[1]Faculty of Life Science, University of Manchester, Manchester M13 9PT, UK

[2]Inflammation and Experimental Surgery Unit, CIBERhed, University Hospital "Virgen de la Arrixaca" - Fundación Formación Investigación Sanitaria Región Murcia, 30120 Murcia, Spain.

[3]Department of Cell Biology and Histology, Faculty of Biology, University of Murcia, 30100 Murcia, Spain.

[4]Hospital Ramón y Cajal, Neurobiology Service, 28034 Madrid, Spain.

Contact: Dr. Pablo Pelegrín, Inflammation and Experimental Surgery Unit, University Hospital "Virgen de la Arrixaca"- Fundación Formación Investigación Sanitaria Región Murcia (FFIS), Carretera Madrid Cartagena s/n, 30120 Murcia, Spain. Tel: 00 34 968 369 317; Fax: 00 34 968 369 364;

e-mail: pablo.pelegrin@ffis.es

Running Title: Cell swelling activates caspase-1

Total character count: 59,909 including spaces.

Summary

Cell volume regulation is a primitive response to alterations in environmental osmolarity. The NLRP3 inflammasome is a multiprotein complex that senses pathogen- and danger-associated signals. Here we report that the basic mechanisms of cell swelling and regulatory volume decrease (RVD) are sensed from fish to mammals by the NLRP3 inflammasome. We found that a decrease in extracellular osmolarity induced (*i*) a K^+-dependent conformational change of the preassembled NLRP3-inactive inflammasome during cell swelling, followed by (*ii*) activation of the NLRP3 inflammasome and caspase-1, which was controlled by Transient Receptor Potential (TRP) channels during RVD. Both mechanisms were necessary for interleukin-1β processing. Increased extracellular osmolarity prevented caspase-1 activation by different known NLRP3 activators. Collectively, our data place cell volume regulation as a basic conserved homeostatic mechanism associated with the formation of the NLRP3 inflammasome and provides a mechanism for NLRP3 inflammasome activation.

Highlights

1. Cell swelling is a conserved danger signal to activate the NLRP3 inflammasome

2. NLRP3 proteins are in pre-assembled inactive complexes before stimulation

3. Activation of NLRP3 inflammasome depends on K^+ efflux and TRP channel stimulation

4. Hypertonic solutions prevent caspase-1 activation in an *in vivo* epileptic model

Introduction

Changes in cell volume have been adapted to function as specific signals to regulate important physiological processes (Hoffmann et al., 2009; Lang et al., 1998). In many physiological conditions, cells exhibit rapid volume regulatory mechanisms to recover their functionality in response to different signals, alterations in osmosensing or osmosignaling are associated with a variety of pathophysiological conditions (Lang et al., 1998). Cell swelling has been reported to occur during different clinical situations such as hypoxia, ischemia, hyponatremia, hypothermia, and in intracellular acidosis and diabetic ketoacidosis (Hoffmann et al., 2009; Newman and Grana, 1988). Cell volume regulation is of prime importance to the central nervous system because of the restricted volume of the skull and current clinical treatment in stroke aims to reduce intracranial pressure by administration of hypertonic solutions (Jain, 2008).

Interleukin-1β (IL-1β) influences the pathogenesis and course of brain diseases such as epilepsies or brain injuries like stroke (Li et al., 2011; Rothwell, 2003). IL-1β release is tightly regulated by the inflammasome, a multi-protein complex that activates caspase-1, the enzyme responsible to generate the mature bioactive form of IL-1β (Schroder and Tschopp, 2010). NLRP3 (Nucleotide-binding, Leucine-rich repeat, Receptor Pyrin 3) oligomerizes and assembles with ASC (Apoptosis-associated Speck-like protein containing a CARD domain) to form functional inflammasomes in response to a wide range of extracellular danger signals including ATP or crystals. The NLRP3 inflammasome is positively regulated by low intracellular K^+, increased reactive oxygen species (ROS) and by lysosome membrane disruption (Hornung et al., 2008; Schroder and Tschopp, 2010; Zhou et al., 2010), processes all affected during cell swelling (Hoffmann et al., 2009). Inflammasomes

do not only regulate immune cells, but they are also functional in other cell types such as neurons, keratinocytes or pancreatic β-cells and generate an integrated host effector response (de Rivero Vaccari et al., 2008; Feldmeyer et al., 2007; Zhou et al., 2010).

An anisosmotic condition represents an important and conserved danger signal, which in the case of hypotonicity, induces processing and release of IL-1β (Perregaux et al., 1996). Recently, it has been reported that activation of NLRP3 inflammasomme by uric acid (MSU) crystal is associated with water influx leading to cell swelling (Schorn et al., 2011). We found that low osmolarities induced macrophage swelling and a decrease of intracellular K^+ and Cl^- concentrations, which activated a regulatory volume decrease process (RVD) controlled by a Transient Receptor Potential (TRP) channel with a pharmacology profile closed to TRP Melastatin 7 (TRPM7). During RVD, TRP Vanilloid 2 (TRPV2) was translocated to the plasma membrane where it induced membrane permeabilization. Then TRP channels modulated intracellular Ca^{2+} rise that was necessary for TGF-β-activated kinase 1 (TAK1) activation. This mechanism showed that low intracellular K^+ is required but not sufficient to induce activation of the NLRP3 inflammasome. Our study gives a molecular target for the currently used hypertonic fluid therapy, and shows that modulation of interstitial osmolarity and TRP inhibition could be beneficial to control inflammatory diseases involving the NLRP3 inflammasome.

Results

Macrophage swelling activates caspase-1 and IL-1β release via the NLRP3 inflammasome

We examined cell volume regulation of macrophages after exposure to changes in extracellular osmolarity. Human THP-1 macrophages responded to a reduction in extracellular osmolarity by cell swelling followed by a regulatory volume decrease (RVD) process to recover their original cellular size (Figure 1A,B). Conversely, an increase in extracellular osmolarity induced macrophage shrinking followed by a regulatory volume increase response (Figure S1A). We made similar observations among different types of mononuclear and other non-immune cells (Figure S1A-C). Recurrent sterile intraperitoneal administration of hypotonic solution in mice induced macrophage swelling *in vivo* (Figure 1C-E) and was sufficient to significantly increase the number of macrophages in peritoneum when compared with isotonic injected animals (Figure 1F).

After *in vitro* LPS priming, a wide range of primary and immortalized human and murine macrophages responded to reduced extracellular osmolarity by releasing caspase-1 dependent cytokines IL-18 and IL-1β (Figure 2A,B and S2A). Such release was not observed when cells were exposed to hypertonic solutions or for tumor necrosis factor-α (TNF-α), a caspase-1 independent cytokine (Figure 2A). The release of IL-1β was abolished with a specific caspase-1 inhibitor (Figure 2C). Active caspase-1 appeared in discrete isolated structures (Figure 2D), suggesting the presence of functional inflammasome-like particles. Contrary to the findings with classical caspase-1 activators (ATP, nigericin, monosodium urate crystals or Aluminum), a hypotonic solution was able to activate caspase-1 in both mammalian

and teleost fish (*Sparus aurata*) macrophages (Figure 2E), both being sensitive to the NLRP3 blocker Bay11-7085 (Juliana et al., 2010) (Figure S2B,C).

In macrophages derived from mice deficient in caspase-1, ASC or NLRP3, IL-1β release following hypotonicity was abolished (Figure 2F and S2D,E) without affecting the RVD response (Figure S2F). In HEK293 cells, expression of NLRP3 inflammasome components demonstrated a requirement of ASC, the Pyrin and the NACHT domain of NLRP3 to activate caspase-1 in response to hypotonic stimulation as well as to the K^+ ionophore nigericin, a classical NLRP3 activator (Figure 2G and S2G).

Macrophage swelling activates NLRP3 preassembled complexes

To examine real time inter-molecular interactions between NLRP3 proteins during cell swelling, we labeled the terminus (C-terminus: Ct or N-terminus: Nt) of these proteins with YFP or Renilla-luciferase (Luc) to record bioluminescence resonance energy transfer (BRET) (Figure 3A). We first demonstrated that our NLRP3-YFP and -Luc tagged proteins were still functional and were able to activate caspase-1 (Figure S3A). Using our validated model of swelling induced inflammasome activation in HEK293 cells (Figure 2G and S1C), we found that prior to stimulation, NLRP3 proteins were in spatial proximity to each other, as a specific saturated BRET signal was found between them (Figure 3B). As a control, the non-interacting protein β-arrestin-YFP gave a non-specific linear increase of the BRET signal with NLRP3-Luc-Ct (Figure 3B). The BRET signal was higher between NLRP3-Luc-Ct and NLRP3-YFP-Nt, than with NLRP3-Luc-Ct and NLRP3-YFP-Ct (Figure 3B), suggesting that in resting NLRP3 complexes the Pyrin-Nt of one NLRP3 protein is in closer proximity to the Ct of adjacent NLRP3 (see proposed model on

Figure 3J). As NLRP3 oligomerization is thought to occur through interaction between central NACHT domains (Schroder and Tschopp, 2010) and deletion of NACHT impairs caspase-1 activation after hypotonic stimulation (Figure S2G), BRET experiments were next performed with NLRP3 constructs deleted for this domain (NLRP3-ΔNACHT). When co-expressed with NLRP3-Luc-Ct, NLRP3-ΔNACHT-YFP-Ct gave a non-specific linear increase of the BRET signal (Figure S3B) confirming the role of NACHT domains in NLRP3 proteins interaction and the specificity of the BRET signal among full-length NLRP3 molecules. Co-expression of ASC with NLRP3 induced an increase of the BRET signal between NLRP3 complexes (Figure 3C). NLRP3 protein interaction was further characterized with biochemical experiments. NLRP3-YFP and NLRP3-Flag proteins co-immunoprecipitated (IP) under both resting conditions, and after a decrease in extracellular osmolarity (Figure 3D), showing that NLRP3 protein interactions were not affected by the stimulation. NLRP3 oligomerization was highly reduced when the NACHT domain of NLRP3 was deleted (Figure S3C).

During the first 5 min after hypotonic stimulation, the magnitude of the BRET signal between NLRP3 proteins was reduced (Figure 3E). This reduction was more pronounced between NLRP3-Luc-Ct and NLRP3-YFP-Nt (Figure 3E) and was absent if cells were maintained in isotonic conditions (Figure S3D). In control samples, we observed no change in the BRET signal after hypotonic stimulation using a Luc-YFP fusion construct (Figure S3E). The decrease in BRET signal observed for NLRP3 proteins during hypotonic shock was also found after nigericin treatment (Figure S3F) and was due to a conformational change in the proteins rather than a dissociation of NLRP3-NLRP3 complexes, since we found similar coIP among NLRP3 proteins before and after hypotonic stimulation (see above, Figure 3D). Conformational

changes in NLRP3 proteins were further confirmed by studying the Flag-tagged immunoprecipitation (Flag IP) efficiency of NLRP3-Flag-Nt proteins. Indeed, less proteins were pulled down after a hypotonic stimulation (Figure 3F,G) without any degradation or release of NLRP3 proteins (Figure S3G,H). The NLRP3 IP efficiency was restored when either NLRP3 proteins were denatured before being pulled down (Figure 3F,G), or when high K^+ concentrations were used during the IP (Figure 3H). As a control, purinergic receptor P2X, ligand-gated ion channel, 7 (P2X7)-Flag IP was not affected by the different K^+ concentrations (Figure 3H). This suggests a K^+-dependent conformational change of NLRP3 after hypotonic stimulation, which could alter the accessibility of the antibody to the Flag epitope. The reduced IP efficiency was more prominent with ASC co-expression (Figure 3G), supporting the idea that ASC is able to compact the Nt of the NLRP3 inflammasome by interacting with its pyrin domain. Despite the evidence of ASC interaction with inactive NLRP3 complexes (Figure 3C,G), direct protein interaction between NLRP3 and ASC was only evident in co-IP experiments after 40 min in hypotonic solution (Figure 3I).

Potassium depletion is not sufficient to activate the NLRP3 inflammasome

We first found that activation of caspase-1 induced by hypotonicity was dependent on intracellular K^+ efflux (Figure 4A-C), as this is an established and obligate step to activate the NLRP3 inflammasome (Schroder and Tschopp, 2010). It is known that cell swelling activates Cl^- efflux in conjunction with K^+ loss to initiate cellular water efflux and maintain cellular homeostasis via RVD (Hoffmann et al., 2009). As expected, macrophage intracellular K^+ concentration decreased during the first 10 min of cell swelling (Figure 4A). Blocking intracellular K^+ depletion by using a hypotonic solution with high concentration of K^+ and glycerol (a membrane

permeable molecule that maintains hypotonicity) still induced cell swelling but abolished the RVD response and the release of mature IL-1β (Figure 4B,C), suggesting that besides K^+ efflux, RVD could be important process to activate the inflammasome. To further investigate the role of RVD in the activation of the inflammasome, we studied the decrease of intracellular Cl^- as a controlling step for the RVD (Figure 4D,E). Using NPPB, a general blocker of swelling-activated Cl^- channels, we found that preventing the RVD response also inhibited the release of mature IL-1β (Figure 4E,F). Interestingly, NPPB did not alter the depletion of intracellular K^+ mediated by cell swelling (Figure 4G). Thus, intracellular K^+ depletion *per se* is necessary but not sufficient to induce swelling-evoked processing and release of IL-1β.

TRP channels regulate caspase-1 activation

We found that in response to hypotonic stimulation macrophages became permeable for large fluorescent molecular tracer (Figure 5A and S4A). This dye uptake occurred during RVD (after 10 min of stimulation) and was not dependent on pannexin-1, P2X7 receptor or caspase-1 activation (Figure S4B,C). We were able to rule out the possible actions of ATP released during cell permeabilization activating the NLRP3 inflammasome, since macrophages deficient of P2X7 receptors, or treatment with apyrase (an enzyme that degrades ATP), did not affect IL-1β release in response to hypotonicity (Figure S4D,E). Treatment with the cathepsin B inhibitor Ca-047-Me, did not impair caspase-1 activation or IL-1β release in response to hypotonicity, so we also ruled out the involvement of cathepsin B in inflammasome activation (Figure S4G-I), even hypotonicity induced lysosome destabilization as measured by cathepsin release (Figure S4F). Hypotonicity induced dye uptake was

sensitive to broad TRP channels blockers (Figure 5A) and TRP inhibition strongly suppressed hypotonic induced caspase-1 activation, IL-1β release, without affecting K^+ efflux in both mammals and fish macrophages (Figure 5B,C and S4J,K). From the TRPs expressed in macrophages (Figure 5D), TRPV2 has been previously identified as an osmosensor and TRPM7 has been involved in controlling the RVD process (Liedtke, 2006; Muraki et al., 2003; Numata et al., 2007). Blocking TRPM7 function by using high extracellular Mg^{++} concentration (Penner and Fleig, 2007) delayed macrophage RVD, decreased cell permeabilization and reduced the release of IL-1β (Figure 5E-G). Similar results were found using broad TRP blockers lanthanum, ruthenium red and 2-APB (Figure 5A,C and S4J,O). Alternatively, the absence of extracellular Mg^{++} potentiate TRPM7 function (Penner and Fleig, 2007) and accelerated RVD, increased cell permeabilization and IL-1β release (Figure 5E-G). Due to the lack of selective antagonists, TRPV2 involvement was studied after silencing in THP-1 using shRNA (Figure S4L,M). TRPV2 gene silencing decreased the dye uptake and the release of IL-1β in response to hypotonic treatment (Figure 5H,I), without affecting the RVD (Figure S4N). As previously described (Nagasawa et al., 2007), we found that macrophage TRPV2 channels were localized on intracellular endosomes (Figure 5J), and were translocated to the plasma membrane after hypotonic stimulation (Figure 5K).

TRP activation modulates intracellular Ca^{2+} and TAK1 phosphorylation

TRP are cationic channels permeable to Ca^{2+}. BAPTA-AM treatment of THP-1 cells completely abolished processing and release of IL-1β in response to hypotonicity (Figure 6A) and intracellular Ca^{2+} variation during cell volume regulation was sensitive to 2-APB (Figure 6B). It has been shown that membrane

stretch and intracellular Ca^{2+} activate TAK1 and this kinase plays a role in NLRP3 inflammasome activation (Fukuno et al., 2011; Gong et al., 2010). We found that a decrease in extracellular osmolarity induced phosphorylation of TAK1 (Figure 6C), which is required for TAK1 activation (Sakurai et al., 2000). Specific inhibition of TAK1 phosphorylation by using 5Z-7-oxozeaenol blocked hypotonicity induced caspase-1 activation and IL-1β processing in a dose dependent manner (Figure 6C) without affecting intracellular K^+ depletion (Figure 6D) or the RVD (Figure 6E). Activation of TAK1 was abolished in the presence of BAPTA-AM (Figure 6C) or when RVD was blocked using NPPB (Figure 6F). Meanwhile, TRP channel inhibitor 2-APB blocked TAK1 phosphorylation (Figure 6G). IL-1β release induced by hypotonicity was also highly reduced in cells where TAK1 gene was silenced (Figure 6H). Altogether, these results show that TAK1 plays a key signaling step downstream TRP channels on NLRP3 inflammasome activation during hypotonic stimulation.

Hypertonic solutions and TRP inhibition prevent the activation of the inflammasome

As a decrease in extracellular osmolarity induced NLRP3 activation, we next determined whether cell volume regulation might be a general mechanism to control NLRP3 inflammasome. Using an *in vivo* model of ear inflammation dependent on the NLRP3 inflammasome activation (Sutterwala et al., 2006; Watanabe et al., 2007) (Figure 7A,B), we found that the size of macrophages was enlarged within the inflamed tissue (Figure 7C,D). The *in vivo* use of 2-APB decreased both ear inflammation and macrophage size (Figure 7A-D), suggesting the importance of the macrophage size and TRP function during inflammation as a feature of cell activation. Also, treatment of macrophages *in vitro* with 2-APB or La^{3+} blocked IL-1β release

induced by classical NLRP3 inflammasome activator as nigericin, *E. coli* or MSU crystals (Figure 7E). Such treatments did not affect IL-1β release induced by DNA mediated AIM2 inflammasome activation (Figure 7E).

As expected, increasing media osmolarity *in vitro* with NaCl, mannitol or sorbitol inhibited hypotonic induced IL-1β release (Figure 7F,G). We also found that hypertonic solutions suppressed NLRP3 inflammasome dependent IL-1β release induced by nigericin, *E. coli*, Alu and MSU crystals (Figure 7F,G), without affecting AIM2 inflammasome activation (Fig. 7G). Hypertonic solutions did not alter K^+ efflux after nigericin treatment (Figure S5B), suggesting that such solutions do not work by affecting K^+ efflux. However, cell swelling and RVD was not a common feature of inflammasome activation, and for example nigericin treatment induced a decrease in intracellular K^+ concentration and cell shrinking without affecting intracellular Cl^- concentration (Figure S5A,C). Macrophages were viable in iso-, hypo- and hyper-tonic solutions and gene expression for NLRP3, ASC and caspase-1 was not affected by these treatments (Figure S5D,E).

We wanted to confirm the *in vivo* relevance of this finding and determine the molecular bases for the current use of hypertonic solutions in clinics during brain inflammation (Jain, 2008). We first found that a hypotonic solution activated caspase-1 in mouse hippocampal neurons in culture (Figure 7H), confirming previous data on functional neuronal caspase-1 (de Rivero Vaccari et al., 2008). As a proof of concept, we used a rat brain injury model induced by injection of kainic acid into the hippocampus to induce cell swelling *in vivo* (Oprica et al., 2003). Microdialysis perfusion of kainic acid in the hippocampus mainly activated caspase-1 in the neurons of the pyramidal layer and dentate gyrus (Figure 7I), and promoted the release of IL-1β (Figure 7J). Both effects, caspase-1 activation and IL-1β release, were reduced by

perfusing a 20% sorbitol hypertonic solution after the administration of kainic acid (Figure 7I,J).

Altogether, our data show cell volume regulation as a basic conserved homeostatic mechanism associated with the formation and stimulation of the NLRP3 inflammasome via TRP channels sensing cell swelling and controlling TAK1 activation.

Discussion

In this study, we found that macrophage swelling induced by hypotonic solutions is a conserved danger signal among vertebrates to activate the NLRP3 inflammasome. This process was dependent on the decrease of intracellular K^+ and Cl^- and a correct RVD process controlled by TRP channels. However, it acted independently of P2X7 receptor signaling and cathepsin B. As already described for others NLRP3 activators, K^+ depletion was a necessary step to induce the activation of the inflammasome. Nevertheless, our study points out that this ionic depletion is not sufficient to induce caspase-1 activation after hypotonicity or nigericin treatment. We also provided molecular mechanistic insights into the assembly and activation of the NLRP3 inflammasome in real time. Finally, our data showed that an increase in extracellular osmolarity abrogated, *in vivo*, caspase-1 activation induced by cell swelling in immune (macrophages) and non-immune (neurons) cells.

Cell volume regulation is an ancient protection mechanism to a change in extracellular osmolarity. During the evolution, this cellular response has been adapted as a signaling pathway involved in many pathophysiological processes (Hoffmann et al., 2009). We found that low osmolarity solutions and cell swelling induced the recruitment of macrophages *in vivo* and could be considered as a potential danger

signal recognized by the immune system. In fact, cell swelling was strongly associated to the activation of macrophages within the inflamed tissue, with caspase-1 activation and the release of IL-1β and IL-18 through the NLRP3 inflammasome. Lower vertebrates and invertebrates present an expanded family of NLR receptors (Hansen et al., 2011), but their function controlling innate immunity is not well understood, since in fish and other lower vertebrates IL-1β sequence lacks a clear caspase-1 processing site (López-Castejón et al., 2008; Pelegrin et al., 2004). In measuring caspase-1 activation, we found that contrary to ATP, nigericin, MSU crystals or Alu, a hypotonic solution was able to activate caspase-1 in both mammalian and fish macrophages. This result places hypotonic environments as an evolutionary alert mechanism conserved from fish to mammalian macrophages to activate caspase-1.

The present model for NLRP3 inflammasome activation is that upon activation, NLRP3 proteins oligomerize and thereby interact with ASC to form a functional multi-protein complex that activates caspase-1 (Jha and Ting, 2009; Schroder and Tschopp, 2010). We used the BRET technique to study in real time inflammasome protein dynamics. Before any stimulation, NLRP3 proteins formed a pre-assembled complex as already described for the NLRP1 inflammasome (Faustin et al., 2007). In this complex, the Pyrin domain of one NLRP3 was in close proximity to the LRR domain of adjacent NLRP3. Self-oligomerization of NLRP3 seems to be mediated by interaction of the NACHT domains, as the BRET signal and co-IP were impaired for NACHT deleted NLRP3 constructs. ASC was able to interact through the Pyrin domain and compact preassembled NLRP3 resting complexes, similarly to what happened during inflammasome activation.

The NLRP3 inflammasome senses a wide range of danger signals, including

extracellular ATP or MSU crystals (Mariathasan et al., 2006; Martinon et al., 2006), however there is no clear common mechanism of NLRP3 activation. Our results demonstrate that a common step is probably membrane stretch, which induces activation of channels (like TRPV2 or pannexin-1) that permeabilize cell membranes (Pelegrin and Surprenant, 2006, 2007). All known activators of the NLRP3 inflammasome induce cell volume changes (swelling or shrinking) (Dise et al., 1980; Schorn et al., 2011; Taylor et al., 2008) and the NLRP3 inflammasome could be a sensor of cellular membrane integrity. Upon hypotonic cell swelling, the decrease in intracellular K^+ concentration carried by activation of mechanosensitive potassium channels, favored a conformational change in NLRP3 proteins by generating the appropriate intracellular environment for the inflammasome activation, probably by increasing electrostatic interactions between NLRP3 proteins as already proposed (Zhang et al., 2011). However, our results rule out intracellular K^+ depletion as the unique cause of caspase-1 activation, because blocking RVD with Cl^--channel or TRP inhibitors abolished release of mature IL-1β without altering cellular K^+ depletion. Moreover, this conclusion was extended to other NLRP3 activators because IL-1β release induced by nigericin was completely blocked by hypertonic solution without affecting K^+ efflux. Both K^+ and Cl^- depletion activated RVD in macrophages as a protection mechanism to elevated membrane tension. Therefore, extracellular osmolarity was sensed by macrophages as a danger signal due to the increase in cellular membrane tension during cell swelling, rather than only a depletion of intracellular K^+ or a direct detection of change in extracellular ionic strength. Indeed, swelling induced by glycerol in a normal sodium-extracellular ionic strength still induced caspase-1 activation. RVD is controlled by the activation of different membrane channels including TRPM7 (Numata et al., 2007). We found that

following cell swelling, a TRP channel with a pharmacology profile similar to TRPM7 (sensitive to ruthenium red, lanthanum, gadolinium, 2-APB and magnesium concentration) regulated the RVD in macrophages. After maximum stretch during cell swelling, endomembranes derived from endosomes and lysosomes are used to repair plasma membrane damages (Togo et al., 2000). In macrophages, we observed that this endomembrane fusion during RVD induced TRPV2 trafficking to the cell surface. As already described for large organic cations, TRPV2 activation is responsible for membrane permeabilization to large molecules (Banke et al., 2010). General blockers of TRP channels abolished RVD (probably controlled by TRPM7), cell permeabilization (due to TRPV2) and caspase-1 activation without altering intracellular K^+ depletion. Cell permeabilization during swelling is also related with the release of cytosolic ATP (Boudreault and Grygorczyk, 2004), which prompts autocrine and/or paracrine purinergic P2X7 receptor signaling and NLRP3 inflammasome activation (Babelova et al., 2009; Iyer et al., 2009; Sanz et al., 2009; Weber et al., 2010). Also, P2X7 induced IL-1β release has been attributed to cell swelling (Perregaux et al., 1996). However, under hypotonic conditions, swelling induced ATP release and P2X7 receptor stimulation were not involved in the activation of NLRP3. Our data show that TRP channel activation modulates intracellular Ca^{2+} during cell volume regulation and this change in intracellular calcium appears to be crucial for the activation of TAK1. A recent study has revealed that TAK1 plays a key role in NLRP3 inflammasome activation (Gong et al., 2010) and that TAK1 might be activated by intracellular Ca^{2+} variations after membrane stretch (Fukuno et al., 2011). We found that, following hypotonic stimulation, TAK1 activation was regulated by TRP activity during RVD and was required for caspase-1 activation and IL-1β processing. We also found that TRP blockers were effective

inhibiting MSU crystal and nigericin induced caspase-1 activation, but the specific involvement of TRPs, and particularly TRPV2, in NLRP3 activation will have to be confirmed by genetic ablation in mouse models (Link et al., 2010).

Hypertonic solutions are used in clinics to reduce brain edema and to reconstitute fluids in patients with trauma or severe sepsis (Jain, 2008; Oliveira et al., 2002). We found that macrophages at inflamed tissues present a characteristic morphology with a considerable increase in cellular volume sensitive to TRP blockers. *In vitro*, hypertonic solutions were able to inhibit the NLRP3 inflammasome in response to different stimuli without affecting IL-1β release induced by AIM2 activation. These results suggest that cellular volume changes specifically modulate activation of the NLRP3 inflammasome towards others inflammatory supramolecular complexes. Although the different NLRP3 stimuli do not directly cause cell swelling (Dise et al., 1980; Taylor et al., 2008), the potential benefit to inhibit the inflammasome activation by inducing cell shrinking using hypertonic solution reinforces the current clinical use of hypertonic osmotherapy to treat different inflammatory diseases (Jain, 2008; Oliveira et al., 2002). To date, the anti-inflammatory beneficial effects of hypertonic solutions were mainly attributed to instantaneous hemodynamic redistribution of interstitial and cellular water into the circulation by the osmotic gradient produced (Diringer and Zazulia, 2004; Oliveira et al., 2002). However, their use to reduce inflammation is highly debated, since no clear molecular mechanism has been attributed to their action. We found that *in vivo*, kainic acid administration activates caspase-1 in neurons and IL-1β release. Perfusion of a hypertonic solution reduced both effects and demonstrates that neuronal cell swelling *in vivo* is also coupled to caspase-1 activation. Although NLRP1 has been proposed as the neuronal inflammasome platform (de Rivero Vaccari et al., 2008), it needs to be

confirmed if *in vivo* kainic acid activates NLRP3 or NLRP1 inflammasome in neurons. These data support previous studies indicating that the activation of caspase-1 could contribute to the pro-inflammatory effects associated to different brain pathologies, like epilepsy or stroke, where neuronal swelling has been reported (de Rivero Vaccari et al., 2008; Rothwell, 2003; Simard et al., 2007).

Altogether, these results reveal that drugs targeting TRP channels or the signaling pathway of cell volume regulatory process are promising tools to reduce inflammation as well as to treat pathologies linked to caspase-1 and NLRP3 activation. Therefore, we propose cell swelling as an evolutionary conserved homeostatic mechanism associated to the formation of NLRP3 inflammasome.

Experimental Procedures

Animals. Male C57BL/6 mice (6-8 weeks old) were obtained from Harlan and maintained in SPF conditions. Healthy specimens (150 g) of the marine fish gilthead seabream (*Sparus aurata*, Actinopterygii, Sparidae) were maintained in 14 m^3 running seawater aquaria. The Local Ethical Committees approved all animal experiments. *P2rx7* deficient mice (Chessell et al., 2005) were from Prof. A. Verkhratsky lab and bone marrow from *Casp1* (Kuida et al., 1995), *Nlrp3* (Martinon et al., 2006) and *Pycard* (Mariathasan et al., 2004) deficient mice were a generous gift of Dr. I. Coullin.

Intraperitoneal administration of hypotonic solution. Mice were treated with daily i.p. injections of 100 ml kg^{-1} of iso- or hypo-tonic solution for 4 consecutive days. 3 h after the last injection, animals were sacrificed and peritoneal cavity was washed. The lavage was analyzed for macrophage size and presence by flow cytometry using anti-F4/80-AlexaFluor488 antibody (Caltag) in a FACScalibur (BD Biosciences). Macrophages population was analyzed using WinList software (Verity Software House).

Kainic acid brain injury model. Brain microdialysis of kainic acid in adult Sprague-Dawley rats aged 10-12 weeks was already described (Hsu et al., 2007; Oprica et al., 2003). Briefly, each hippocampus was stereotaxicaly (AP: -4.6 mm; L: ±2.6 mm from bregma; V: 2.6 mm from dura) implanted with a CMA/12 microdialysis probe (CMA/microdialysis), after 2 h washout, 100 μM kainic acid was perfused for 1 h (flow 1 μl/min) followed by the infusion of isotonic Krebs-Ringer bicarbonate (KRB) solution (280-290 mOsm) in one hippocampus, and hypertonic KRB supplemented

with 20% sorbitol (1400-1500 mOsm) in the contralateral side. Samples for IL-1β analysis were collected every hour for 8 h. At the end of the experiment the biotinylated caspase-1 inhibitor (100 μm biotinyl-YVAD-CMK, Anaspec) was perfused for 1 h. 12 h later, animals were sacrificed, and brains were removed for immunohistochemical studies.

Cells, treatments and procedures. Mouse primary BMDM, peritoneal macrophages, immortalized mouse BMDM, fish macrophages, THP-1 and HEK293 cell culture was described previously (Hornung et al., 2008; López-Castejón et al., 2008; Lopez-Castejon et al., 2010; Pelegrin and Surprenant, 2009). For details of hippocampal cultures, human macrophage isolation and BRET measurements, see Supplemental Information. If not specified, all macrophages were primed for 4 h with LPS (1 μg/ml) previous to hypotonic solution challenge. For TRPV2 gene silencing, THP-1 cells were infected with recombinant lentivirus vectors and experiments were performed seven days after infection. For TAK1 gene silencing, THP-1 cells were cultured in presence of *Accell* TAK1 siRNA or *Accell* non-targeting siRNA pool (Thermo Scientific Dharmacon) for 72 h according to manufacturer's instruction. If not mentioned in the text, all the hypo- and iso-tonic solutions had an osmolarity of 90 and 300 mOsm respectively. 90 mOsm hypotonic solution was achieved by diluting isotonic physiology Et-buffer (Pelegrin and Surprenant, 2009) 1:4 with distilled sterile water.

Detailed methods for qRT-PCR, RT-PCR, immunocytochemistry, microscopy, Western blots, IP, LDH measurements, ELISA, cathepsin release, dye uptake, plasma membrane biotynilation, FLICA staining, have been previously described (López-Castejón et al., 2008; Lopez-Castejon et al., 2010; Pelegrin and Surprenant, 2009).

Intracellular K^+ concentration was analyzed on a Hitachi-917 (Roche). Macrophage area measurements were quantified from >50 cells/condition/time-point using NIH ImageJ software (http://rsb.info.nih.gov/ij).

Statistical analysis. All data are shown as mean values and error bars represent SEM from the number of assays indicated (from at least three independent experiments). For statistical comparisons, data were analyzed by an unpaired two-tailed Student's t-test to determine difference between groups using Prism software (Graph-Pad Software, Inc.), *p* value is indicated in the legend of the Figures.

Acknowledgements

We thank I. Couillin for *Casp1*, *Pycard* and *Nlrp3* deficient mice bone marrow, A. Verkhratsky for *P2rx7* receptor deficient mice and E. Latz for immortalized BMDM from C57BL/6, *Pycard* and *Nlrp3* deficient mice. We thank J. Tschopp for NLRP3-flag, G. Dubyak for ASC-V5, J. Perroy for Luc-YFP and J.P. Pin for β-arrestin-YFP expression vectors. We thank O. Fernandez for advice with animal models, L. Martinez-Alarcón for human blood extraction, F. Machado-Linde for collecting human peritoneal lavages, F. Noguera for running Hitachi ion detection system, P.J. Martínez for animal handling, E. Moutin for hippocampal neurons culture and E. Martin, R. Gaskell, I. Fuentes and M.C. Baños for both molecular and cellular technical assistance. We would like to thank A. Surprenant and F. Rassendren for helpful discussions and support. We are in debt with R.A. North, D. Brough, L.E. Browne and O. Stelmashenko for critical revision of the manuscript. V. Compan is supported by grant from Wellcome Trust. This work was supported by grants from PN I+D+I 2008-2011-Instituto Salud Carlos III-FEDER (EMER07/049 and PI09/0120), Fundación Séneca (11922/PI/09), managed by Fundación Formación Investigación Sanitaria Región de Murcia (FFIS), grants from Spanish Ministry of Science and Technology (BIO2008-01379, BIO2011-23400) and *Fundación Marcelino Botín*.

Author Contributions

V.C. contributed to design, execution, analysis and interpretation of *in vitro* experiments of Figures 1B, 2C,D,G, 3A-I, 4B,C,E,F, 5A,C,F,H,I-K, 6C,F-H, 7H. A.B-M. and C.M.M. performed and analyzed *in vivo* models of Figures 1C-F, 7A-D. A.B-M., G.L-C. and A.I.G. performed and analyzed experiments of Figures 1A,

2A,B,F, 4A,D,G, 5B,D,E,G, 6A,B,D,E, 7E-G. D.A. and V.M. designed, performed and analyzed fish experiments of Figure 2E. M.T.M., A.S.H., E.B. and D.R. designed, performed, analyzed and interpreted the kainic acid model of Figure 7I,J. P.P. conceived, designed and supervised this study, analyzed and interpreted results and wrote the final manuscript with V.C. and contributions from the other authors.

References

Babelova, A., Moreth, K., Tsalastra-Greul, W., Zeng-Brouwers, J., Eickelberg, O., Young, M.F., Bruckner, P., Pfeilschifter, J., Schaefer, R.M., Gröne, H.-J., and Schaefer, L. (2009). Biglycan, a danger signal that activates the NLRP3 inflammasome via toll-like and P2X receptors. J Biol Chem *284*, 24035-24048.

Banke, T.G., Chaplan, S.R., and Wickenden, A.D. (2010). Dynamic changes in the TRPA1 selectivity filter lead to progressive but reversible pore dilation. Am J Physiol-Cell Ph *298*, C1457-1468.

Boudreault, F., and Grygorczyk, R. (2004). Cell swelling-induced ATP release is tightly dependent on intracellular calcium elevations. The Journal of Physiology *561*, 499-513.

Chessell, I.P., Hatcher, J.P., Bountra, C., Michel, A.D., Hughes, J.P., Green, P., Egerton, J., Murfin, M., Richardson, J., Peck, W.L.*, et al.* (2005). Disruption of the P2X7 purinoceptor gene abolishes chronic inflammatory and neuropathic pain. Pain *114*, 386-396.

de Rivero Vaccari, J.P., Lotocki, G., Marcillo, A.E., Dietrich, W.D., and Keane, R.W. (2008). A molecular platform in neurons regulates inflammation after spinal cord injury. J Neurosci *28*, 3404-3414.

Diringer, M.N., and Zazulia, A.R. (2004). Osmotic therapy: fact and fiction. Neurocrit Care *1*, 219-233.

Dise, C.A., Goodman, D.B., and Rasmussen, H. (1980). Selective stimulation of erythrocyte membrane phospholipid fatty acid turnover associated with decreased cell volume. J Biol Chem *255*, 5201-5207.

Faustin, B., Lartigue, L., Bruey, J.-M., Luciano, F., Sergienko, E., Bailly-Maitre, B., Volkmann, N., Hanein, D., Rouiller, I., and Reed, J.C. (2007). Reconstituted NALP1

inflammasome reveals two-step mechanism of caspase-1 activation. Molecular Cell *25*, 713-724.

Feldmeyer, L., Keller, M., Niklaus, G., Hohl, D., Werner, S., and Beer, H.-D. (2007). The inflammasome mediates UVB-induced activation and secretion of interleukin-1beta by keratinocytes. Curr Biol *17*, 1140-1145.

Fukuno, N., Matsui, H., Kanda, Y., Suzuki, O., Matsumoto, K., Sasaki, K., Kobayashi, T., and Tamura, S. (2011). TGF-beta-activated kinase 1 mediates mechanical stress-induced IL-6 expression in osteoblasts. Biochem Biophys Res Commun *408*, 202-207.

Gong, Y.-N., Wang, X., Wang, J., Yang, Z., Li, S., Yang, J., Liu, L., Lei, X., and Shao, F. (2010). Chemical probing reveals insights into the signaling mechanism of inflammasome activation. Cell Res *20*, 1289-1305.

Hansen, J.D., Vojtech, L.N., and Laing, K.J. (2011). Sensing disease and danger: A survey of vertebrate PRRs and their origins. Dev Comp Immunol *35*, 886-897.

Hoffmann, E.K., Lambert, I.H., and Pedersen, S.F. (2009). Physiology of cell volume regulation in vertebrates. Physiological Reviews *89*, 193-277.

Hornung, V., Bauernfeind, F., Halle, A., Samstad, E.O., Kono, H., Rock, K.L., Fitzgerald, K.A., and Latz, E. (2008). Silica crystals and aluminum salts activate the NALP3 inflammasome through phagosomal destabilization. Nat Immunol *9*, 847-856.

Hsu, Y.H., Lee, W.T., and Chang, C. (2007). Multiparametric MRI evaluation of kainic acid-induced neuronal activation in rat hippocampus. Brain *130*, 3124-3134.

Iyer, S.S., Pulskens, W.P., Sadler, J.J., Butter, L.M., Teske, G.J., Ulland, T.K., Eisenbarth, S.C., Florquin, S., Flavell, R.A., Leemans, J.C., and Sutterwala, F.S. (2009). Necrotic cells trigger a sterile inflammatory response through the Nlrp3 inflammasome. Proc Natl Acad Sci USA *106*, 20388-20393.

Jain, K.K. (2008). Neuroprotection in traumatic brain injury. Drug Discov Today *13*, 1082-1089.

Jha, S., and Ting, J.P. (2009). Inflammasome-associated nucleotide-binding domain, leucine-rich repeat proteins and inflammatory diseases. J Immunol *183*, 7623-7629.

Juliana, C., Fernandes-Alnemri, T., Wu, J., Datta, P., Solorzano, L., Yu, J.-W., Meng, R., Quong, A.A., Latz, E., Scott, C.P., and Alnemri, E.S. (2010). Anti-inflammatory compounds parthenolide and Bay 11-7082 are direct inhibitors of the inflammasome. J Biol Chem *285*, 9792-9802.

Kuida, K., Lippke, J.A., Ku, G., Harding, M.W., Livingston, D.J., Su, M.S., and Flavell, R.A. (1995). Altered cytokine export and apoptosis in mice deficient in interleukin-1 beta converting enzyme. Science *267*, 2000-2003.

Lang, F., Busch, G.L., Ritter, M., Volkl, H., Waldegger, S., Gulbins, E., and Haussinger, D. (1998). Functional significance of cell volume regulatory mechanisms. Physiol Rev *78*, 247-306.

Li, G., Bauer, S., Nowak, M., Norwood, B., Tackenberg, B., Rosenow, F., Knake, S., Oertel, W.H., and Hamer, H.M. (2011). Cytokines and epilepsy. Seizure *20*, 249-256.

Liedtke, W. (2006). Transient receptor potential vanilloid channels functioning in transduction of osmotic stimuli. J Endocrinol *191*, 515-523.

Link, T.M., Park, U., Vonakis, B.M., Raben, D.M., Soloski, M.J., and Caterina, M.J. (2010). TRPV2 has a pivotal role in macrophage particle binding and phagocytosis. Nat Immunol *11*, 232-239.

López-Castejón, G., Sepulcre, M.P., Mulero, I., Pelegrin, P., Meseguer, J., and Mulero, V. (2008). Molecular and functional characterization of gilthead seabream Sparus aurata caspase-1: the first identification of an inflammatory caspase in fish. Mol Immunol *45*, 49-57.

Lopez-Castejon, G., Theaker, J., Pelegrin, P., Clifton, A.D., Braddock, M., and Surprenant, A. (2010). P2X7 Receptor-Mediated Release of Cathepsins from Macrophages Is a Cytokine-Independent Mechanism Potentially Involved in Joint Diseases. J Immunol *185*, 2611-2619.

Mariathasan, S., Newton, K., Monack, D.M., Vucic, D., French, D.M., Lee, W.P., Roose-Girma, M., Erickson, S., and Dixit, V.M. (2004). Differential activation of the inflammasome by caspase-1 adaptors ASC and Ipaf. Nature *430*, 213-218.

Mariathasan, S., Weiss, D.S., Newton, K., McBride, J., O'Rourke, K., Roose-Girma, M., Lee, W.P., Weinrauch, Y., Monack, D.M., and Dixit, V.M. (2006). Cryopyrin activates the inflammasome in response to toxins and ATP. Nature *440*, 228-232.

Martinon, F., Pétrilli, V., Mayor, A., Tardivel, A., and Tschopp, J. (2006). Gout-associated uric acid crystals activate the NALP3 inflammasome. Nature *440*, 237-241.

Muraki, K., Iwata, Y., Katanosaka, Y., Ito, T., Ohya, S., Shigekawa, M., and Imaizumi, Y. (2003). TRPV2 is a component of osmotically sensitive cation channels in murine aortic myocytes. Circulation Research *93*, 829-838.

Nagasawa, M., Nakagawa, Y., Tanaka, S., and Kojima, I. (2007). Chemotactic peptide fMetLeuPhe induces translocation of the TRPV2 channel in macrophages. J. Cell. Physiol. *210*, 692-702.

Newman, P.J., and Grana, W.A. (1988). The changes in human synovial fluid osmolality associated with traumatic or mechanical abnormalities of the knee. Arthroscopy *4*, 179-181.

Numata, T., Shimizu, T., and Okada, Y. (2007). TRPM7 is a stretch- and swelling-activated cation channel involved in volume regulation in human epithelial cells. Am J Physiol-Cell Ph *292*, C460-467.

Oliveira, R.P., Velasco, I., Soriano, F.G., and Friedman, G. (2002). Clinical review: Hypertonic saline resuscitation in sepsis. Critical care (London, England) *6*, 418-423.

Oprica, M., Eriksson, C., and Schultzberg, M. (2003). Inflammatory mechanisms associated with brain damage induced by kainic acid with special reference to the interleukin-1 system. J Cell Mol Med *7*, 127-140.

Pelegrin, P., Chaves-Pozo, E., Mulero, V., and Meseguer, J. (2004). Production and mechanism of secretion of interleukin-1beta from the marine fish gilthead seabream. Dev Comp Immunol *28*, 229-237.

Pelegrin, P., and Surprenant, A. (2006). Pannexin-1 mediates large pore formation and interleukin-1beta release by the ATP-gated P2X7 receptor. EMBO J *25*, 5071-5082.

Pelegrin, P., and Surprenant, A. (2007). Pannexin-1 couples to maitotoxin- and nigericin-induced interleukin-1beta release through a dye uptake-independent pathway. J Biol Chem *282*, 2386-2394.

Pelegrin, P., and Surprenant, A. (2009). Dynamics of macrophage polarization reveal new mechanism to inhibit IL-1beta release through pyrophosphates. EMBO J *28*, 2114-2127.

Penner, R., and Fleig, A. (2007). The Mg2+ and Mg(2+)-nucleotide-regulated channel-kinase TRPM7. Handb Exp Pharmacol, 313-328.

Perregaux, D.G., Laliberte, R.E., and Gabel, C.A. (1996). Human monocyte interleukin-1beta posttranslational processing. Evidence of a volume-regulated response. J Biol Chem *271*, 29830-29838.

Rothwell, N. (2003). Interleukin-1 and neuronal injury: mechanisms, modification, and therapeutic potential. Brain, Behavior, and Immunity *17*, 152-157.

Sakurai, H., Miyoshi, H., Mizukami, J., and Sugita, T. (2000). Phosphorylation-dependent activation of TAK1 mitogen-activated protein kinase kinase kinase by TAB1. FEBS Lett *474*, 141-145.

Sanz, J.M., Chiozzi, P., Ferrari, D., Colaianna, M., Idzko, M., Falzoni, S., Fellin, R., Trabace, L., and Di Virgilio, F. (2009). Activation of microglia by amyloid {beta} requires P2X7 receptor expression. J Immunol *182*, 4378-4385.

Schorn, C., Frey, B., Lauber, K., Janko, C., Strysio, M., Keppeler, H., Gaipl, U.S., Voll, R.E., Springer, E., Munoz, L.E.*, et al.* (2011). Sodium overload and water influx activate the NALP3 inflammasome. J Biol Chem *286*, 35-41.

Schroder, K., and Tschopp, J. (2010). The inflammasomes. Cell *140*, 821-832.

Simard, J.M., Kent, T.A., Chen, M., Tarasov, K.V., and Gerzanich, V. (2007). Brain oedema in focal ischaemia: molecular pathophysiology and theoretical implications. Lancet Neurol *6*, 258-268.

Sutterwala, F.S., Ogura, Y., Szczepanik, M., Lara-Tejero, M., Lichtenberger, G.S., Grant, E.P., Bertin, J., Coyle, A.J., Galán, J.E., Askenase, P.W., and Flavell, R.A. (2006). Critical role for NALP3/CIAS1/Cryopyrin in innate and adaptive immunity through its regulation of caspase-1. Immunity *24*, 317-327.

Taylor, S.R.J., Gonzalez-Begne, M., Dewhurst, S., Chimini, G., Higgins, C.F., Melvin, J.E., and Elliott, J.I. (2008). Sequential shrinkage and swelling underlie P2X7-stimulated lymphocyte phosphatidylserine exposure and death. J Immunol *180*, 300-308.

Togo, T., Krasieva, T.B., and Steinhardt, R.A. (2000). A decrease in membrane tension precedes successful cell-membrane repair. Mol Biol Cell *11*, 4339-4346.

Watanabe, H., Gaide, O., Pétrilli, V., Martinon, F., Contassot, E., Roques, S., Kummer, J.A., Tschopp, J., and French, L.E. (2007). Activation of the IL-1beta-

processing inflammasome is involved in contact hypersensitivity. J Investig Dermatol *127*, 1956-1963.

Weber, F.C., Esser, P.R., Müller, T., Ganesan, J., Pellegatti, P., Simon, M.M., Zeiser, R., Idzko, M., Jakob, T., and Martin, S.F. (2010). Lack of the purinergic receptor P2X7 results in resistance to contact hypersensitivity. J Exp Med *207*, 2609-2619.

Zhang, Z., Witham, S., and Alexov, E. (2011). On the role of electrostatics in protein-protein interactions. Phys Biol *8*, 035001.

Zhou, R., Tardivel, A., Thorens, B., Choi, I., and Tschopp, J. (2010). Thioredoxin-interacting protein links oxidative stress to inflammasome activation. Nat Immunol *11*, 136-140.

Figure Legends

Figure 1 Hypotonic solutions are considered as danger signals *in vivo*. A, Time lapse images of THP-1 cells in a hypotonic solution (90 mOsm), initial volume (white dotted line) and maximum volume (black dotted line) are indicated; scale bar 5 μm. **B,** Relative cell area of THP-1 cells in isotonic (continuous trace) or hypotonic (dotted trace) solution. *n* = 50 cells per condition and representative of 4 independent experiments. **C,** Representative flow cytometry forward scatter (FSC-H) plots of mouse F4/80 positive cells in the peritoneum of mice injected for 4 days with an iso- or hypotonic solution. **D,E,** Percentage of high-FSC-H (D) and mean of FCS-H (E) gated F4/80 positive peritoneal cells as shown in C. *n* = 3 animals per condition. **F,** Percentage of F4/80 positive cells in the peritoneum of mice injected for 4 days with an iso- (*n* = 6 animals, white circles) or hypotonic (*n* = 9 animals, black circles) solution. **p < 0.005, *p < 0.05. See also Figure S1.

Figure 2 Macrophage swelling induces release of IL-1β and activation of caspase-1 via NLRP3-inflammasome. A, ELISA of released IL-1β (blue trace), IL-18 (red trace) or TNF-α (black trace) and Western blot analysis of mature IL-1β released by THP-1 cells primed or not with LPS (1 μg/ml, 4 h) and subsequently subjected to different extracellular osmolarities for 1h; *ns*: no significant difference compared with isotonic conditions. *n* = 3 independent experiments. Maximum concentration of IL-1β, IL-18 and TNF-α was 12.5±0.58, 1.94±0.11 and 1.49±0.19 ng/ml respectively. **B,** ELISA of IL-1β release by different macrophages (Mϕs) treated as described in A. Human macrophages were: THP-1, primary peritoneal macrophages (Per) and peripheral blood monocytes (HPBM); and mouse macrophages were: primary peritoneal macrophages (Per) and bone marrow-derived macrophages (BMDM). *n* =

3-7 independent experiments. **C,** Western blot analysis of the cleavage of pro-IL-1β to its active p17 form (IL-1β) and of caspase-1 to its active p10 subunit by THP-1 treated as described in A in the presence or absence of the caspase-1 inhibitor (Ac-YVAD-AOM, 100 μM); *C*: cell lysates and *SN*: supernatants. **D,** Representative high-resolution, deconvolved images of mouse peritoneal macrophages treated as described in A, stained with fluorescent probe for active caspase-1 (FLICA, green) and F-actin cytoskeleton stained with Texas Red-phalloidin (red); scale bar 2,5 μm. The inserts show staining of a population of >15 cells. **E,** Caspase-1 activity measured in fish macrophages (grey bars) or mouse BMDM (white bars) after hypotonic media stimulation (Hypo, 1h), ATP (5 mM, 30 min), nigericin (1 μM, 30 min mammalian and 1 h fish), MSU crystals (500 μg/ml, 1h) or Alu crystals (500 μg/ml mammalian and 40 μg/ml for fish, 1h); n = 3 to 4 independent experiments. **F,** ELISA of IL-1β release by bone marrow-derived wild-type (WT), Caspase-1-deficient (*Casp1*$^{-/-}$), ASC-deficient (*Pycard*$^{-/-}$) or NLRP3-deficient (*Nlrp3*$^{-/-}$) macrophages treated as described in A or with 3 mM ATP for 30 min; n = 3 independent cultures. **G,** Western blot analysis of the cleavage of pro-caspase-1 to its active p10 subunit in HEK293 cells transfected with pro-caspase-1 and NLRP3; pro-caspase-1, NLRP3 and ASC; or pro-caspase-1, NLRP3-PYR-deletion and ASC, incubated for 1 h with hypotonic solution or 30 min with nigericin (5 μM). **p < 0.001. See also Figure S2.

Figure 3 NLRP3 proteins form an inactive preassembled complex in resting cells. **A,** Schematic representation showing NLRP3 BRET donor and acceptor partners. **B,** BRET saturation curves for HEK293 cells transfected with a constant concentration of NLRP3-Luc-Ct and increasing amounts of the BRET acceptor NLRP3-YFP-Nt (black circles), NLRP3-YFP-Ct (open circles) or β-arrestin-YFP (grey triangles). **C,**

BRET signal from HEK293 cells transfected with NLRP3-Luc-Ct and NLRP3-YFP-Ct in the presence or absence of ASC co-expression; **p < 0.001. **D,** NLRP3-YFP and NLRP3-flag co-IP in resting conditions or after hypotonic stimulation in HEK293 cells (*C*: cell lysates). Western blots are representative of 3 independent experiments. **E,** Kinetics of net BRET signal in HEK293 cells transfected with the BRET donor NLRP3-Luc-Ct and the acceptors NLRP3-YFP-Nt (black circles) or -Ct (open circles) in response to hypotonic solution. **F-H,** NLRP3-flag or P2X7-flag IP after hypotonic stimulation in HEK293. IP were performed on naive or denatured (SDS+DTT) lysates **(F)** and in the presence of different concentrations of K^+ **(H)**. Histograms in **G** are the densitometry quantification of the NLRP3-falg IP signal after hypotonic stimulation of 3 independent blots in the absence or the presence of ASC co-transfection. **I,** Kinetic of co-IP between ASC and NLRP3-flag in HEK293 cells after hypotonic stimulation; *C*: total cell lysate. Western blots are representative of 2 to 3 independent experiments. **J,** Proposed model for the intermolecular dynamics of NLRP3 inflammasome activation in response to hypotonicity. See also Figure S3.

Figure 4 RVD controls activation of the NLRP3 inflammasome. A, Relative intracellular K^+ concentration of THP-1 primed with LPS (1 µg/ml, 4 h) and subsequently subjected to 300 or 90 mOsm extracellular solution for 1 h; n = 3 independent experiments. **B,** Relative cell area of THP-1 cells in isotonic solution (continuous trace) or in hypotonic solutions (dotted trace) composed of 120 mM glycerol (dotted trace) and either 140 mM of NaCl (open squares) or 140 mM of KCl (black circles); n = 50 cells per treatment and representative of 3 independent experiments. **C,** Western blot analysis of the cleavage of pro-IL-1β to its active p17 form (IL-1β) and of β-actin by LPS primed THP-1 incubated for 1 h with a 90

mOsmol hypotonic solution (Hypos.) or in hypotonic solutions composed of 120 mM glycerol and either 140 mM NaCl (Na^+ Gly) or 140 mM of KCl (K^+ Gly). *C*: cell lysates, *SN*: supernatants. **D,** Relative intracellular Cl^- concentration of THP-1 treated as in A; n = 3 independent experiments. **E,** Relative cell area of THP-1 cells in isotonic solution (continuous trace) or in 90 mOsm solution (dotted line) in the absence (open squares) or presence of 100 μM NPPB (closed circles). **F,** Western blot analysis of the cleavage of pro-IL-1β to its active p17 form (IL-1β) on THP-1 treated as in A in the presence or absence of NPPB (100 μM). **G,** Relative intracellular K^+ concentration of THP-1 treated as in A in the presence or absence of NPPB (100 μM). Western blots are representative of 2 to 3 independent experiments. **$p < 0.001$.

Figure 5 TRP channels control caspase-1 activation during RVD. A, Kinetic of Yo-Pro uptake in THP-1 during hypotonicity in the absence or presence of $LaCl_3$ (La, 2 mM), 2-APB (100 μM), ruthenium red (RR, 100 μM) or $GdCl_3$ (Gd, 2 mM); average traces of 3 independent experiments. **B,** Relative intracellular K^+ concentration of THP-1 treated as described in A; n = 3 independent experiments. **C,** Western blot analysis of the cleavage of pro-IL-1β to its active p17 form (IL-1β) and of caspase-1 to its active p10 subunit by THP-1 treated as described in A; *C*: cell lysates, *SN*: supernatants. **D,** RT-qPCR of TRP channel family expression in THP-1, human peritoneal macrophages (hPer) and blood monocytes (HPBM). **E,** Relative cell area of THP-1 cells in 90 mOsm solution with different concentrations of Mg^{++}. **F,** Kinetic of Yo-Pro uptake in THP-1 cells during hypotonic solution stimulation with different concentrations of Mg^{++}; average traces of 3 independent experiments. **G,** ELISA of released IL-1β by THP-1 cells primed with LPS (1 μg/ml, 4 h) and subsequently subjected to different extracellular osmolarities for 1h with different

concentrations of Mg^{++}; *n* = 6 independent experiments. **H,** Kinetic of Yo-Pro uptake in THP-1 cells infected with GFP-lentivirus (GFP-Lv) or with shTRPV2-lentivirus (TRPV2-shRNA) during hypotonic solution stimulation; average traces of 3 independent experiments. **I,** Western blot analysis of β-actin and of the cleavage of pro-IL-1β to its active p17 form (IL-1β) by THP-1 infected as described in H; *C*: cell lysates, *SN*: supernatants. **J,** High-resolution, deconvolved images of TRPV2 and EEA1 immunostaining on mouse peritoneal macrophages; scale bar 2,5 μm. **K,** TRPV2-myc or P2X2-myc plasma membrane biotinylation (top panels), total cell lysate immunoblot (middle panels) or TRPV2-myc immunostaining (bottom panels) on HEK293 cells treated for 40 min with iso- or hypo-tonic solution; scale bar 2,5 μm, arrowhead denotes TRPV2 membrane localization. *p < 0.05; **p < 0.005. See also Figure S4.

Figure 6 TRP channels modulate macrophage intracellular Ca^{2+} and TAK1 activation. A, Western blot analysis of the cleavage of pro-IL-1β to its active p17 form (IL-1β) by THP-1 primed with LPS (1 μg/ml, 4 h) and subsequently subjected to 300 or 90 mOsm extracellular solution for 1 h, in the presence or absence of BAPTA-AM (100 μM). **B,** Intracellular Ca^{2+} changes of THP-1 treated as in A in the presence or absence of 2-APB (100 μM), BAPTA-AM (100 μM) or an extracellular buffer without calcium (EGTA). **C**, Western blot analysis of TAK1 phosphorylation, and the cleavage of pro-IL-1β to its active p17 form (IL-1β) and of caspase-1 to its active p10 subunit by THP-1 treated as in A in the presence or absence of different concentrations of 5Z-7-oxozeaenol (OXO) or BAPTA-AM (100 μM). **D**, Relative intracellular K^+ concentration of THP-1 primed as in C; *n* = 3 independent experiments. **E**, Relative cell area of THP-1 cells treated as in C. *n* = 50 cells per

condition. **F,G**, Western blot analysis of TAK1 phosphorylation and the cleavage of pro-IL-1β to its active p17 form (IL-1β) by THP-1 treated as in A in the presence or absence of NPPB (100 μM, **F**) or 2-APB (100 μM, **G**). **H**, Western blot analysis of TAK1 phosphorylation, β-actin and the cleavage of pro-IL-1β to its active p17 form (IL-1β) by THP-1 silenced or not for TAK1 gene, following hypotonic stimulation.

Figure 7 Inflammation is blocked by TRP inhibition or hypertonic solutions. A, Representative histology of mouse ear inflammatory model induced with AITC in the presence of absence of 2-APB (100 μM); representative from 5 different animals; scale bar 40 μm. **B,** Measurements of ear inflammation (*n* = 25 sections per condition). **C,** Measurement of F4/80 positive macrophage size inside the inflamed ear tissue (*n* = 30 to 60 macrophages per condition). **D,** Representative histology of mouse ear macrophage; scale bar 20 μm. **E-G,** IL-1β release detected by ELISA (E,G) or Western blot (F) in THP-1 primed for 4 h with LPS (1 μg/ml) and treated with hypotonic solution (90 mOsm, Hypos. or Hyposmotic), nigericin (25 μM, Nig), Alu (500 mg/ml), MSU (500 mg/ml), *E. coli* challenge or lipofectamine-DNA complexes (DNA). When indicated the buffer was supplemented with 2-APB (100 μM), $LaCl_3$ (La, 2 mM), NaCl (150 mM), sorbitol (20%) or mannitol (20%); *n* = 3 to 4 independent experiments. **H,** Representative images of hippocampal mouse neurons in culture, treated with a hypotonic solution for 30 min, stained with fluorescent probe for active caspase-1 (FLICA, green), MAP2 (red) and DAPI; scale bar 20 μm (left and middle panels) and 10 μm (right panels). **I,** Histochemical detection of active caspase-1 in the rat hippocampus after administration of 100 μM kainate in isotonic or hypertonic solution (Krebs-Ringer bicarbonate solution supplemented with 20% of sorbitol). Active caspase-1 (green) co-localizes with NeuN-positive neurons (insert,

red) of the pyramidal layer (PL) and the dentate gyrus (GD); scale bar 100 μm. **J,** ELISA of IL-1β release in the hippocampus of rats after administration of 100 μM kainate in iso- (red trace) or hyper- (blue trace) tonic solution, n = 4 animals per treatment. ***p< 0.001,**p < 0.005, *p < 0.05. See also Figure S5.

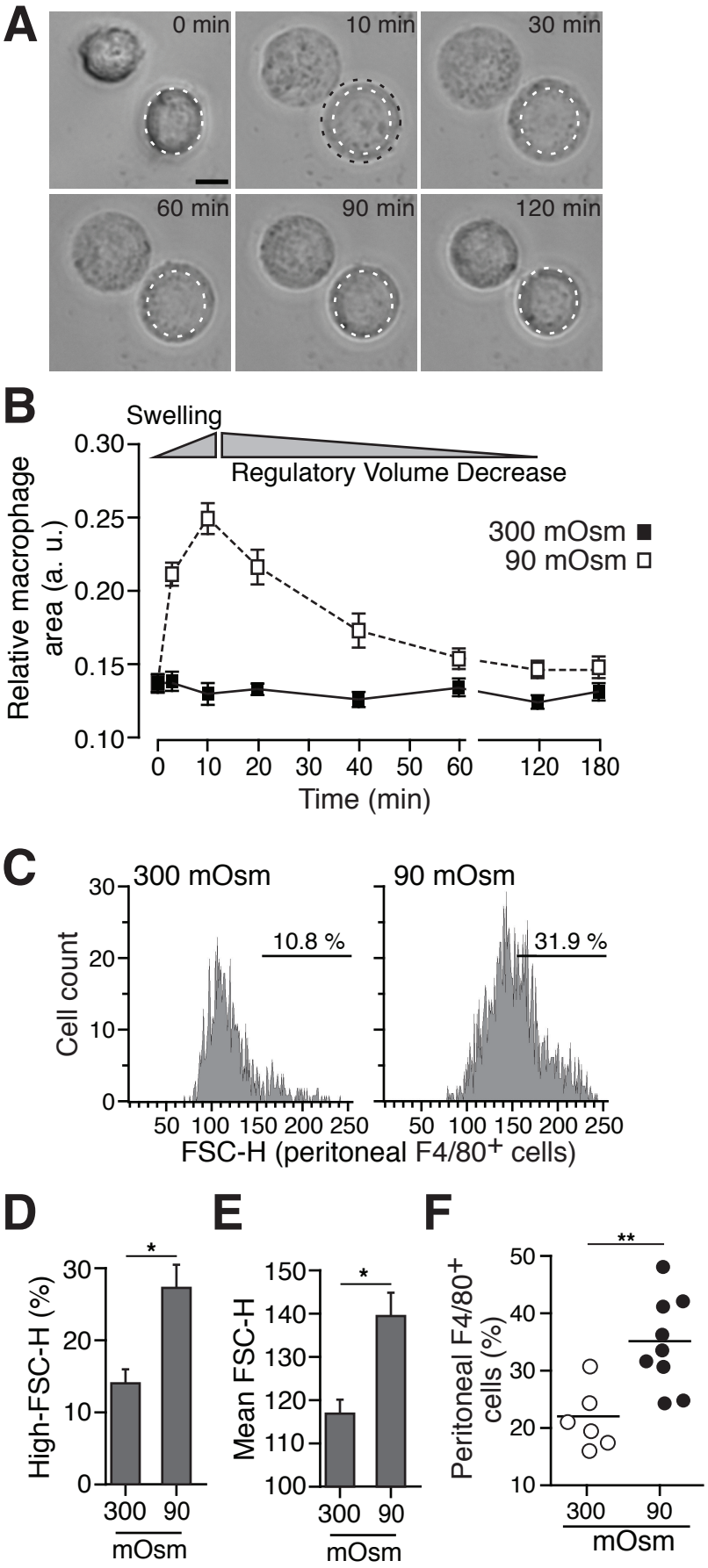
A
0 min
10 min
30 min
60 min
90 min
120 min
B
Swelling
Regulatory Volume Decrease
Relative macrophage area (a. u.)
0.30
0.25
0.20
0.15
0.10
300 mOsm
90 mOsm
0 10 20 30 40 50 60 120 180
Time (min)
C
300 mOsm
90 mOsm
10.8 %
31.9 %
Cell count
30
20
10
0
50 100 150 200 250
50 100 150 200 250
FSC-H (peritoneal F4/80+ cells)
D
High-FSC-H (%)
*
30
20
10
0
300 90
mOsm
E
Mean FSC-H
*
150
140
130
120
110
100
300 90
mOsm
F
Peritoneal F4/80+ cells (%)
**
50
40
30
20
10
300 90
mOsm

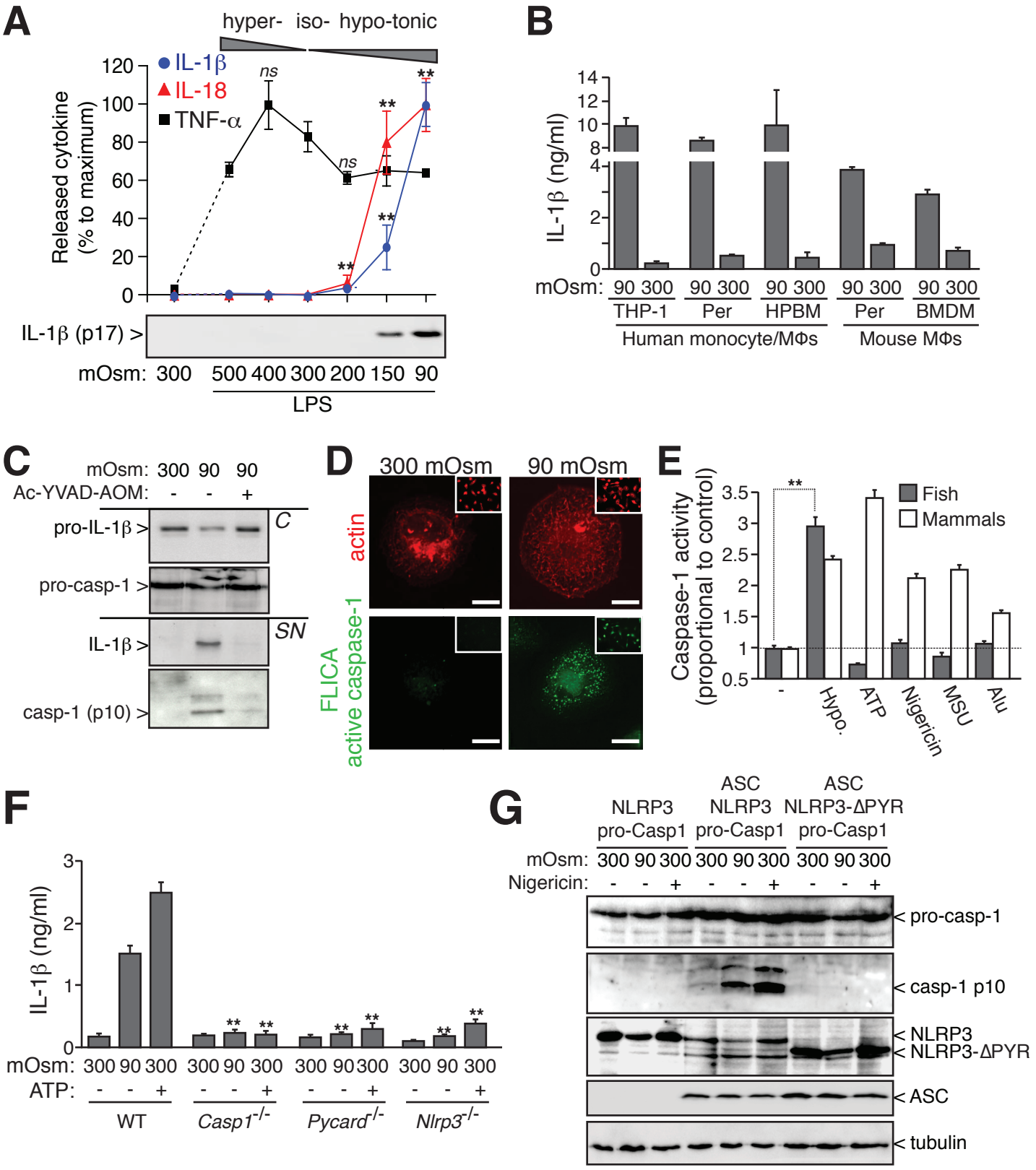
A
hyper- iso- hypo-tonic
IL-1β
IL-18
TNF-α
Released cytokine (% to maximum)
ns
**
IL-1β (p17) >
mOsm: 300 500 400 300 200 150 90
LPS
B
IL-1β (ng/ml)
mOsm: 90 300 90 300 90 300 90 300 90 300
THP-1 Per HPBM Per BMDM
Human monocyte/MΦs
Mouse MΦs
C
mOsm: 300 90 90
Ac-YVAD-AOM: - - +
pro-IL-1β >
pro-casp-1 >
IL-1β >
casp-1 (p10) >
C
SN
D
300 mOsm
90 mOsm
actin
FLICA active caspase-1
E
Caspase-1 activity (proportional to control)
Fish
Mammals
-
Hypo.
ATP
Nigericin
MSU
Alu
F
IL-1β (ng/ml)
mOsm: 300 90 300 300 90 300 300 90 300 300 90 300
ATP: - - + - - + - - + - - +
WT
Casp1-/-
Pycard-/-
Nlrp3-/-
G
NLRP3 pro-Casp1
ASC NLRP3 pro-Casp1
ASC NLRP3-ΔPYR pro-Casp1
mOsm: 300 90 300 300 90 300 300 90 300
Nigericin: - - + - - + - - +
pro-casp-1
casp-1 p10
NLRP3
NLRP3-ΔPYR
ASC
tubulin

Figure 3

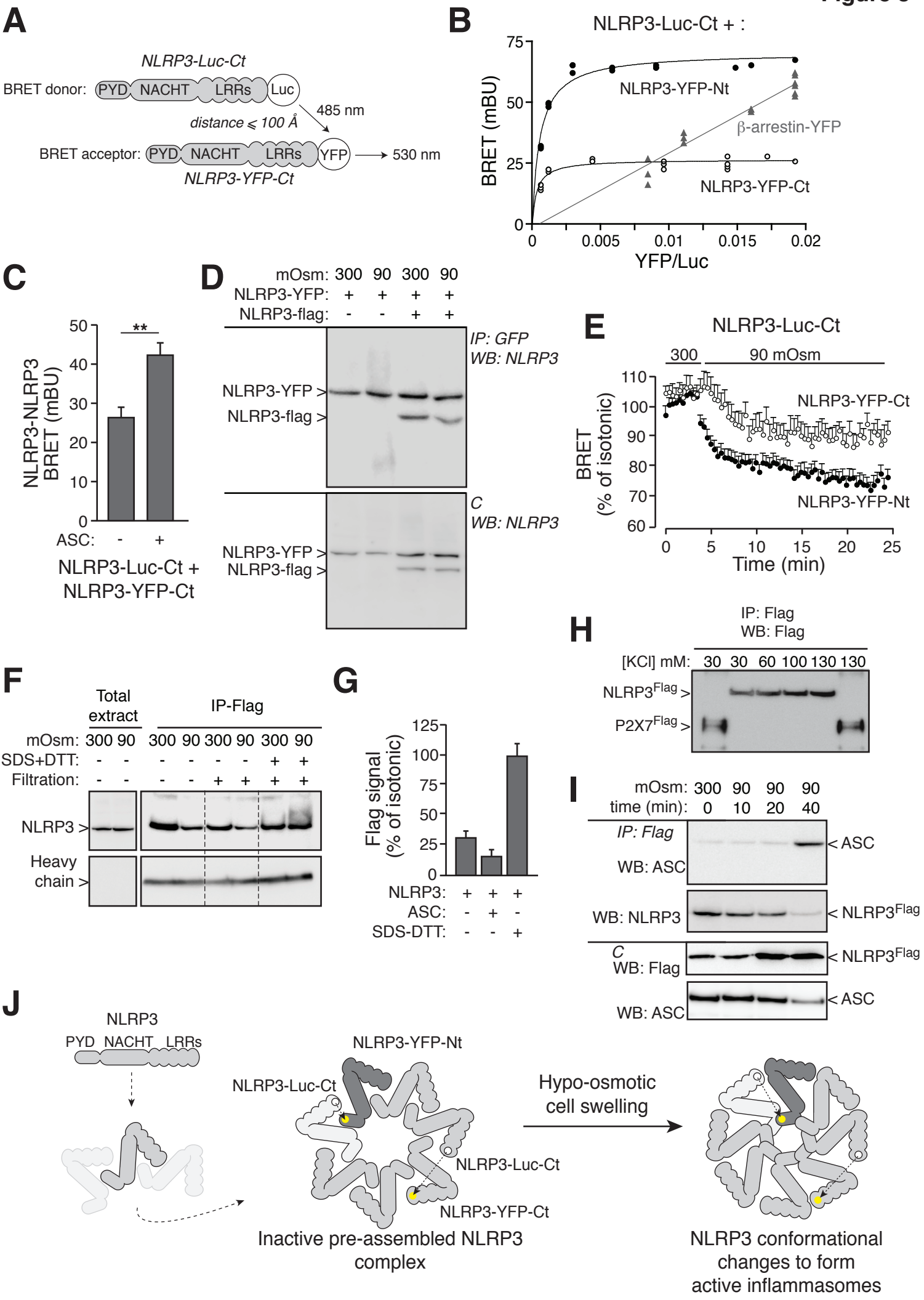
A
NLRP3-Luc-Ct
BRET donor:
PYD
NACHT
LRRs
Luc
485 nm
distance ⩽ 100 Å
BRET acceptor:
PYD
NACHT
LRRs
YFP
530 nm
NLRP3-YFP-Ct
B
NLRP3-Luc-Ct + :
BRET (mBU)
NLRP3-YFP-Nt
β-arrestin-YFP
NLRP3-YFP-Ct
YFP/Luc
C
NLRP3-NLRP3 BRET (mBU)
**
ASC:
NLRP3-Luc-Ct +
NLRP3-YFP-Ct
D
mOsm:
NLRP3-YFP:
NLRP3-flag:
IP: GFP
WB: NLRP3
NLRP3-YFP
NLRP3-flag
C
WB: NLRP3
E
NLRP3-Luc-Ct
300
90 mOsm
BRET (% of isotonic)
NLRP3-YFP-Ct
NLRP3-YFP-Nt
Time (min)
F
Total extract
IP-Flag
mOsm:
SDS+DTT:
Filtration:
NLRP3
Heavy chain
G
Flag signal (% of isotonic)
NLRP3:
ASC:
SDS-DTT:
H
IP: Flag
WB: Flag
[KCl] mM:
NLRP3Flag
P2X7Flag
I
mOsm:
time (min):
IP: Flag
WB: ASC
ASC
WB: NLRP3
NLRP3Flag
C
WB: Flag
NLRP3Flag
WB: ASC
ASC
J
NLRP3
PYD NACHT LRRs
NLRP3-YFP-Nt
NLRP3-Luc-Ct
NLRP3-Luc-Ct
NLRP3-YFP-Ct
Inactive pre-assembled NLRP3 complex
Hypo-osmotic cell swelling
NLRP3 conformational changes to form active inflammasomes

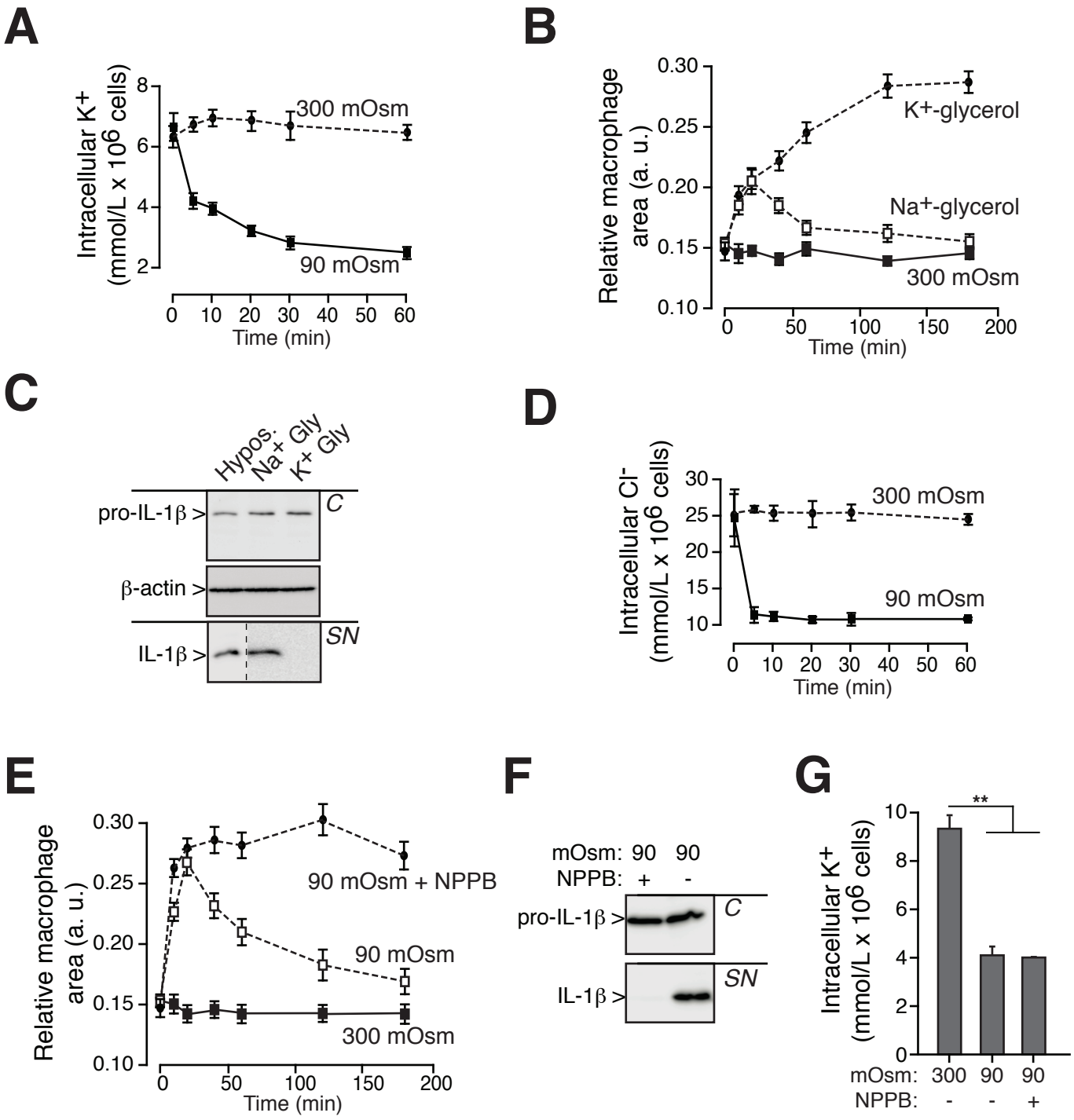
A
Intracellular K+ (mmol/L x 10^6 cells)
300 mOsm
90 mOsm
Time (min)
B
Relative macrophage area (a. u.)
K+-glycerol
Na+-glycerol
300 mOsm
Time (min)
C
Hypos:
Na+ Gly
K+ Gly
pro-IL-1β
β-actin
IL-1β
C
SN
D
Intracellular Cl- (mmol/L x 10^6 cells)
300 mOsm
90 mOsm
Time (min)
E
Relative macrophage area (a. u.)
90 mOsm + NPPB
90 mOsm
300 mOsm
Time (min)
F
mOsm: 90 90
NPPB: + -
pro-IL-1β
IL-1β
C
SN
G
Intracellular K+ (mmol/L x 10^6 cells)
**
mOsm: 300 90 90
NPPB: - - +

Figure 5

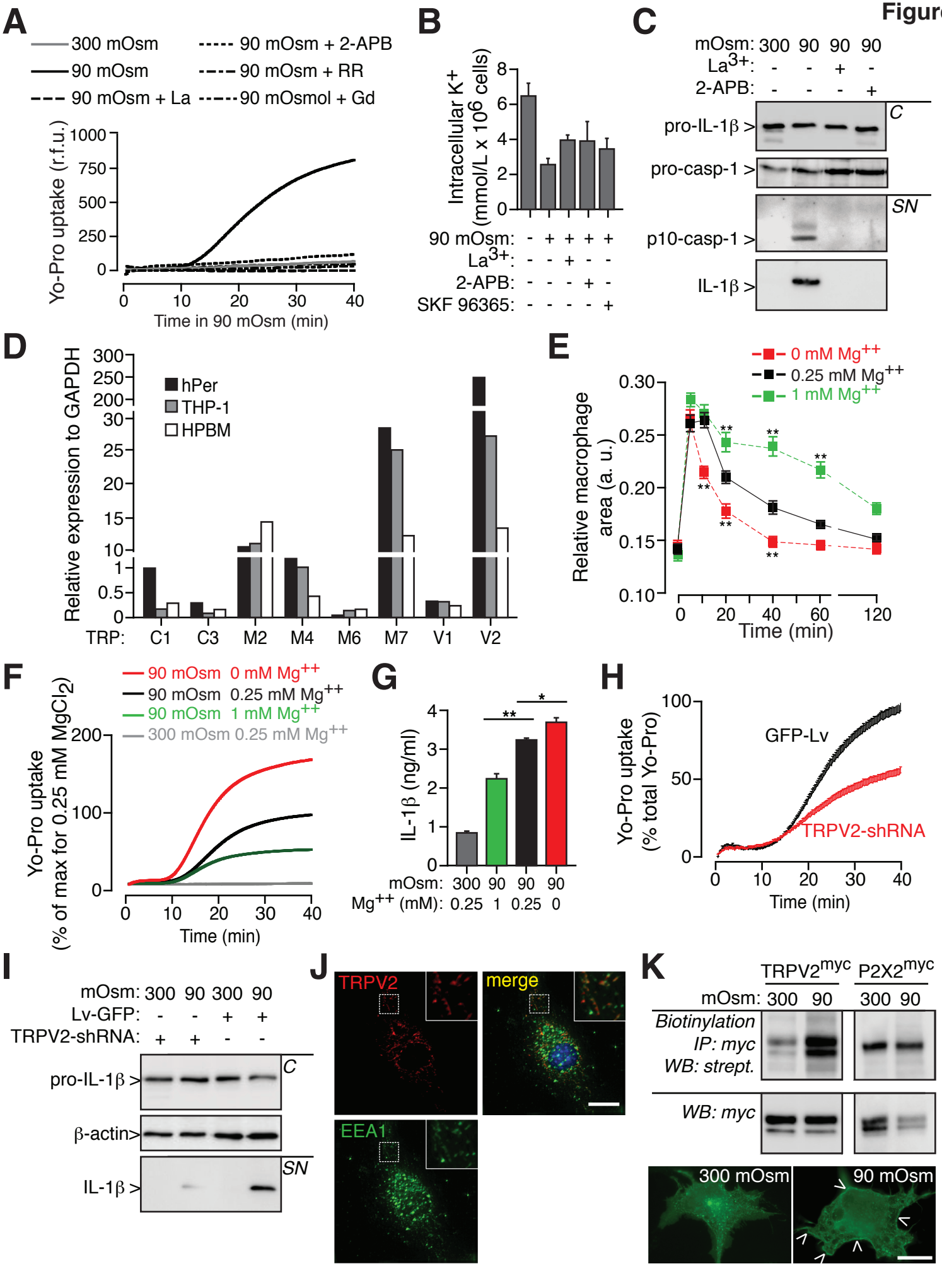
A
300 mOsm
90 mOsm
90 mOsm + La
90 mOsm + 2-APB
90 mOsm + RR
90 mOsmol + Gd
Yo-Pro uptake (r.f.u.)
Time in 90 mOsm (min)
B
Intracellular K+ (mmol/L x 10^6 cells)
90 mOsm:
La3+:
2-APB:
SKF 96365:
C
mOsm: 300 90 90 90
La3+: - - + -
2-APB: - - - +
pro-IL-1β >
pro-casp-1 >
p10-casp-1 >
IL-1β >
C
SN
D
Relative expression to GAPDH
hPer
THP-1
HPBM
TRP: C1 C3 M2 M4 M6 M7 V1 V2
E
0 mM Mg++
0.25 mM Mg++
1 mM Mg++
Relative macrophage area (a. u.)
Time (min)
F
90 mOsm 0 mM Mg++
90 mOsm 0.25 mM Mg++
90 mOsm 1 mM Mg++
300 mOsm 0.25 mM Mg++
Yo-Pro uptake (% of max for 0.25 mM MgCl2)
Time (min)
G
IL-1β (ng/ml)
mOsm: 300 90 90 90
Mg++ (mM): 0.25 1 0.25 0
H
GFP-Lv
TRPV2-shRNA
Yo-Pro uptake (% total Yo-Pro)
Time (min)
I
mOsm: 300 90 300 90
Lv-GFP: - - + +
TRPV2-shRNA: + + - -
pro-IL-1β >
β-actin>
IL-1β >
C
SN
J
TRPV2
merge
EEA1
K
TRPV2myc
P2X2myc
mOsm: 300 90 300 90
Biotinylation
IP: myc
WB: strept.
WB: myc
300 mOsm
90 mOsm

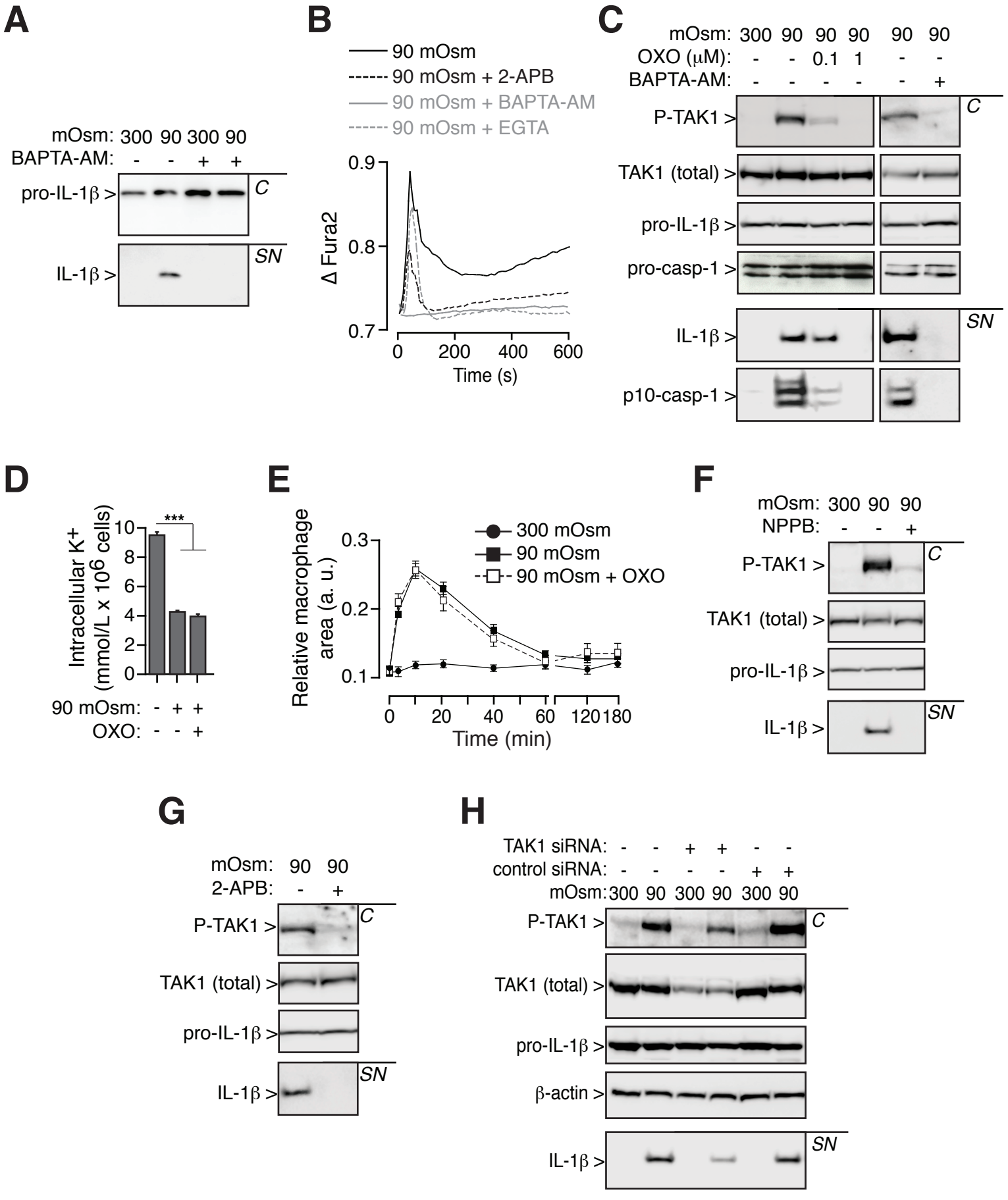
A
mOsm: 300 90 300 90
BAPTA-AM: - - + +
pro-IL-1β >
C
IL-1β >
SN
B
90 mOsm
90 mOsm + 2-APB
90 mOsm + BAPTA-AM
90 mOsm + EGTA
Δ Fura2
0.9
0.8
0.7
0
200
400
600
Time (s)
C
mOsm: 300 90 90 90 90 90
OXO (μM): - - 0.1 1 - -
BAPTA-AM: - - - - - +
P-TAK1 >
C
TAK1 (total) >
pro-IL-1β >
pro-casp-1 >
IL-1β >
SN
p10-casp-1 >
D
Intracellular K+ (mmol/L x 10^6 cells)
10
8
6
4
2
0
***
90 mOsm: - + +
OXO: - - +
E
Relative macrophage area (a. u.)
0.3
0.2
0.1
300 mOsm
90 mOsm
90 mOsm + OXO
0
20
40
60
120
180
Time (min)
F
mOsm: 300 90 90
NPPB: - - +
P-TAK1 >
C
TAK1 (total) >
pro-IL-1β >
IL-1β >
SN
G
mOsm: 90 90
2-APB: - +
P-TAK1 >
C
TAK1 (total) >
pro-IL-1β >
IL-1β >
SN
H
TAK1 siRNA: - - + + - -
control siRNA: - - - - + +
mOsm: 300 90 300 90 300 90
P-TAK1 >
C
TAK1 (total) >
pro-IL-1β >
β-actin >
IL-1β >
SN

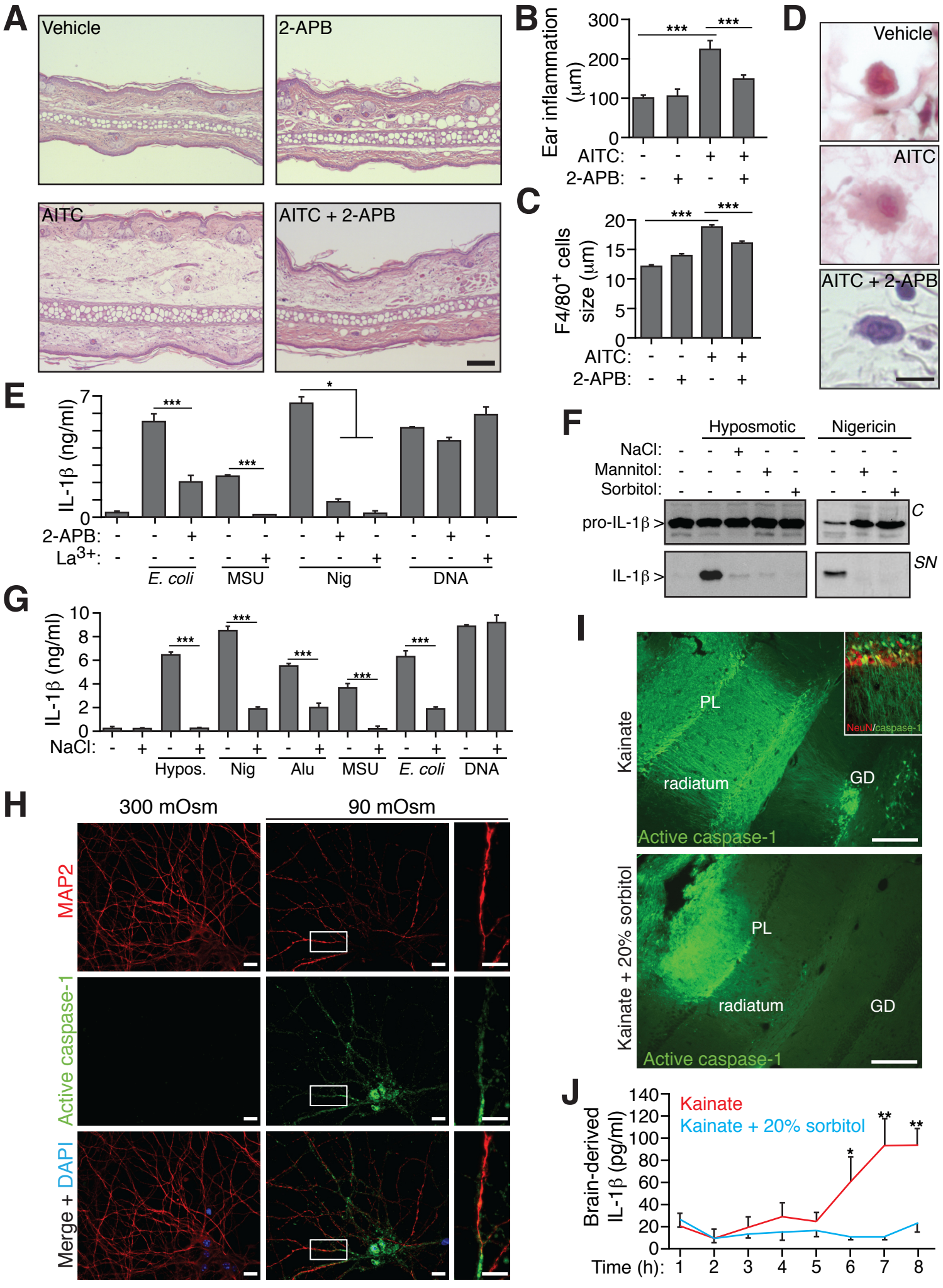
A
Vehicle
2-APB
AITC
AITC + 2-APB
B
Ear inflammation (μm)
300
200
100
0
***
***
AITC: - - + +
2-APB: - + - +
C
F4/80+ cells size (μm)
20
15
10
5
0
***
***
AITC: - - + +
2-APB: - + - +
D
Vehicle
AITC
AITC + 2-APB
E
IL-1β (ng/ml)
7
0
***
***
*
2-APB: - - + - - - + - - + -
La3+: - - - - + - - + - - +
E. coli
MSU
Nig
DNA
F
Hyposmotic
Nigericin
NaCl: - - + - - - - -
Mannitol: - - - + - - + -
Sorbitol: - - - - + - - +
pro-IL-1β >
C
IL-1β >
SN
G
IL-1β (ng/ml)
10
8
6
4
2
0
***
***
***
***
***
NaCl: - + - + - + - + - + - +
Hypos.
Nig
Alu
MSU
E. coli
DNA
H
300 mOsm
90 mOsm
MAP2
Active caspase-1
Merge + DAPI
I
Kainate
PL
radiatum
GD
NeuN/caspase-1
Active caspase-1
Kainate + 20% sorbitol
PL
radiatum
GD
Active caspase-1
J
Brain-derived IL-1β (pg/ml)
140
120
100
80
60
40
20
0
Kainate
Kainate + 20% sorbitol
*
**
**
Time (h): 1 2 3 4 5 6 7 8